

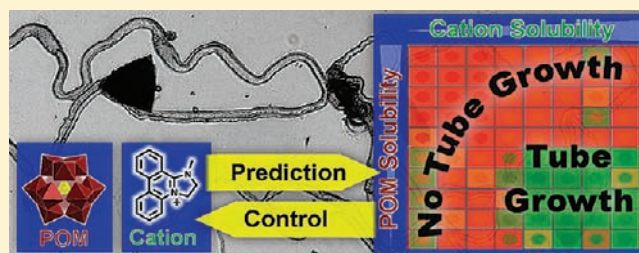
# Osmotically Driven Crystal Morphogenesis: A General Approach to the Fabrication of Micrometer-Scale Tubular Architectures Based on Polyoxometalates

Geoffrey J. T. Cooper, Antoine G. Boulay, Philip J. Kitson, Chris Ritchie, Craig J. Richmond, Johannes Thiel, David Gabb, Roslyn Eadie, De-Liang Long, and Leroy Cronin\*

School of Chemistry, WestCHEM, The University of Glasgow, University Avenue, Glasgow G12 8QQ, U.K.

**S** Supporting Information **W** Web-Enhanced

**ABSTRACT:** The process of osmotically driven crystal morphogenesis of polyoxometalate (POM)-based crystals is investigated, whereby the transformation results in the growth of micrometer-scale tubes 10–100  $\mu\text{m}$  in diameter and many thousands of micrometers long. This process initiates when the crystals are immersed in aqueous solutions containing large cations and is governed by the solubility of the parent POM crystal. Evidence is presented that indicates the process is general to all types of POMs, with solubility of the parent crystal being the deciding parameter. A modular approach is adopted since different POM precursor crystals can form tubular architectures with a range of large cationic species, producing an ion-exchanged material that combines the large added cations and the large POM-based anions. It is also shown that the process of morphogenesis is electrostatically driven by the aggregation of anionic metal oxides with the dissolved cations. This leads to the formation of a semi-permeable membrane around the crystal. The osmotically driven ingress of water leads to an increase in pressure, and ultimately rupture of the membrane occurs, allowing a saturated solution of the POM to escape and leading to the formation of a “self-growing” microtube in the presence of the cation. It is demonstrated that the growth process is sustained by the osmotic pressure within the membrane surrounding the parent crystal, as tube growth ceases whenever this pressure is relieved. Not only is the potential of the modular approach revealed by the fact that the microtubes retain the properties of their component parts, but it is also possible to control the direction of growth and tube diameter. In addition, the solubility limits of tube growth are explored and translated into a predictive methodology for the fabrication of tubular architectures with predefined physical properties, opening the way for real applications.



## INTRODUCTION

The re-fabrication of material architectures through morphogenesis from one form to another *via* the transformation of crystalline materials,<sup>1</sup> aggregation of nanoparticles,<sup>2</sup> interfacial self-assembly of polymers,<sup>3</sup> and amphiphilic systems<sup>4</sup> (or combinations of these) can allow the assembly of novel structures spanning the nano, mesoscale and beyond.<sup>5</sup> In these systems, the organization of matter under non-equilibrium conditions,<sup>6</sup> ruled by dissipative processes,<sup>7</sup> is vital since it allows the assembly of complex new architectures, based upon a modular approach, and with novel physicochemical properties.<sup>8</sup>

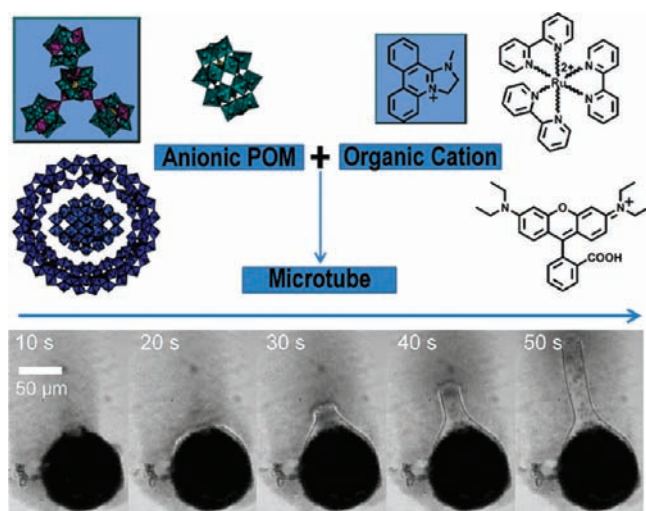
In chemistry today, one of the most exciting and least understood areas revolves around manipulating complex non-equilibrium chemical systems, especially if the non-equilibrium process can be manipulated during the fabrication of new materials.<sup>6</sup> Such materials can continue to grow/be fabricated as long as the system is sustained far from equilibrium while the fluxes are maintained, leading to the emergence of temporal and spatial structures. Key chemical examples are the Belousov–Zhabotinsky (BZ) reaction,<sup>9</sup> where an oscillating chemical reaction in a thin film can give rise to

temporal pattern formation, and crystal gardens,<sup>10–13</sup> which yield spatially defined structures formed by seeding a saturated silicate solution with a crystal of a transition metal salt. Although these systems are very interesting and form a range of temporally defined patterns, a vast amount of research has already been carried out, and they are still poorly understood, as it is difficult to construct controllable examples in the laboratory to allow systematic studies.<sup>12</sup> In this respect, we opted to examine the self-assembly of a class of polymeric metal oxides, in the hope that robust architectures can be formed and manipulated.

Polyoxometalates (POMs) are discrete molecular oxides of early transition metals with a wide range of applications from catalysis<sup>14,15</sup> and material science<sup>16–18</sup> to medicine.<sup>19</sup> Their synthesis generally involves the self-assembly of dissolved transition metal oxides through condensation and reduction mechanisms, which can be controlled by an organic cation<sup>20–23</sup> or an inorganic seed in a templating role, using “one-pot” conditions.<sup>24</sup>

**Received:** December 7, 2010

**Published:** March 29, 2011

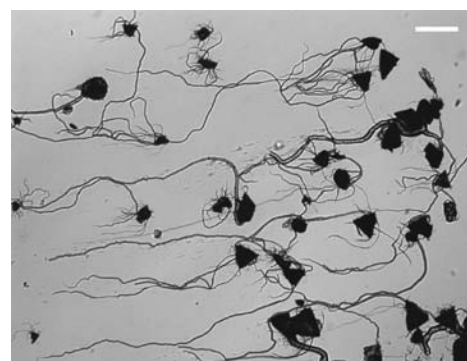


**Figure 1.** Scheme showing how several POMs and either aromatic cations or transition metal complexes can interact to form microtubes. The original couple<sup>26</sup> (POM I/compound 1; see Tables 1 and 2) that led to the discovery is highlighted. The POM is used in crystalline form and immersed in an aqueous solution containing the cations in a known concentration. The rate of growth is investigated using time-lapse photography using an optical microscope equipped with a CCD camera.

Under such conditions, the control of the assembly of the POM cluster is often defined by the precise reaction conditions; a large variety of species are formed which can be considered to be members of a dynamic library generated *in situ*. However, by maintaining reactions in far from equilibrium states using a constant flow of dissolved precursors, we are able to access different materials, including intermediate species, and this can be interesting for “selecting” given members of a library.<sup>24</sup>

In a preliminary study, by us, it has been shown that microtubes can be spontaneously grown from crystals of POM-based materials<sup>25</sup> when immersed in solutions containing dihydroimidazophenanthridinium (DIP) cations (Figure 1) with variable growth rates (1–100  $\mu\text{m}/\text{s}$ ) and vast aspect ratios (>1000: 1).<sup>26</sup> Not only do the tubes remain hollow after growth has ceased, but their diameter and direction of growth can be controlled in real time, allowing complex pre-designed patterns to be realized.<sup>27</sup>

The transformation of the crystals into the tubular architectures appears to occur when a solution of a bulky cation on a sparsely soluble crystal allows it to dissolve locally and produce a hollow membrane mediated by the electrostatically driven aggregation of the POM crystal and the bulky cation added to the solution, which produces an insoluble matrix. Once this permeable membrane is formed, water can pass through and the osmotic pressure inside increases. When the system reaches a critical pressure, the membrane ruptures and the dissolved POM material that is contained within the membrane is ejected through the aperture, whereupon it comes into contact with the cation solution, leading to further aggregation (see movie 1 showing this process). The aggregate is composed of the cations and POM anions bound electrostatically in a charge-balancing ratio.<sup>27</sup> Since water ingress at the crystal maintains a constant outflow of material through the opening, closure of the structure is not possible, and the aggregation produces extended tubular architectures. This process is able to transform a large number of crystals simultaneously (see Figure 2).



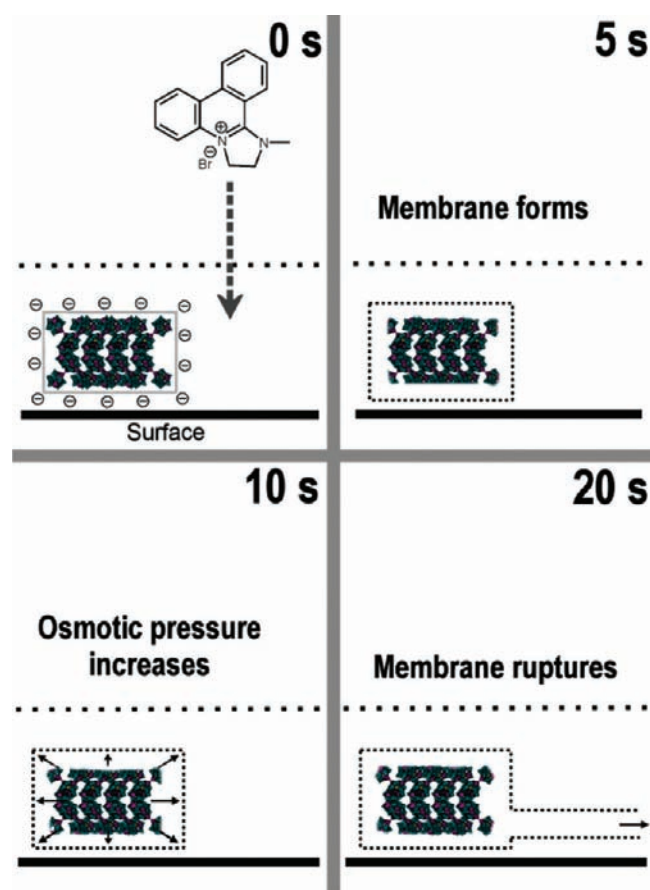
**Figure 2.** Picture of a large number of crystals that have all been transformed from crystalline form to crystals that have sprouted very long tubes on addition of large cations to the aqueous solution (POM I/compound 1; see Tables 1 and 2) in which the tubes are immersed. The photograph was taken 15 min after cation addition. Tubes have grown in a uniform direction due to a bulk flow of solvent in this system (from right to left). The white scale bar is 500  $\mu\text{m}$  long.

The flow of the POM-based solution is sustained while crystalline material is still present in the parent membrane and continues to be dissolved. Consequently, the osmotic engine still pumps water and the system is kept in flux, resulting in continued tube growth until the material housed within the crystal is completely expended. If, for any reason, the flux is weakened or stopped, the tube growth stops immediately.

Herein, it is established that this phenomenon is not limited to one POM compound but can be generalized over the entire family of molecular metal oxides, as well as reporting key mechanistic data. Specifically, an extensive study is presented with a large range of POM materials and cations, including transition metal complexes, and demonstrates the solubility dependencies of tube growth. These data have allowed us to substantiate our proposed mechanism for tube growth, as well as to develop a new methodology for the design of POM-based tubular architectures with predefined properties, opening the way for the design of device architectures and development of new applications. The development of the new methodology is dependent upon understanding the critical solubility parameters that govern the ability of the different POM/cation combinations to produce tubes. An assay of 10 different POM materials and 8 cationic species was carried out to show the robustness and modularity of the POM-based tubular architectures and to correlate the rate of growth and the average diameter of the tubes with the concentration of the solution and the chemical characteristics of the starting materials. In addition, it is observed that the transition metal complexes containing polyaromatic ligands such as 2,2'-bipyridine or 1,10-phenanthroline are also able to act as a cation during the tube growth process, and this opens the way for the development of truly modular systems, combining functionality from both the POM anion and the added cation. Finally, it is shown that tubes can be “artificially” extruded from a needle and that a minimal “seed” of a single POM crystal coated in an appropriate cation can grow tubes when introduced to pure water.

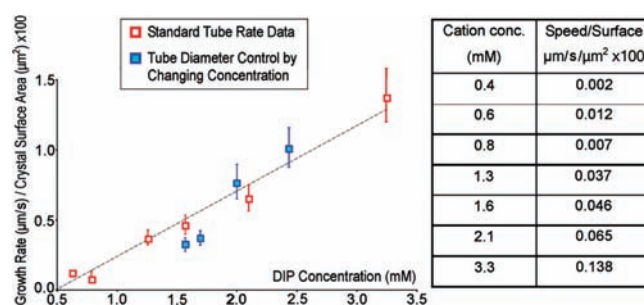
## RESULTS AND DISCUSSION

Ever since we first reported the spontaneous growth of POM-based tubular architectures from a crystalline POM sample



**Figure 3.** Scheme detailing the general mechanism involved in tube growth. A membrane (shown as a dotted line) is formed by electrostatic interaction between the dissolved POM and the organic cations dissolved in solution. Water comes through the porous membrane, and the increase of internal pressure leads to rupture, whereupon tubes start to grow.

during an exchange reaction with a large organic cation,<sup>26</sup> we have been trying to define the critical parameters that control tube growth and exploring the mechanism in order to potentially exploit the process of crystal-based morphogenesis to develop new material architectures with desired applications. Until our report this process was unknown, although there are some mechanistic parallels with the growth processes in crystal garden formation,<sup>10,11</sup> which can provide a useful guide for investigating this phenomenon. In the formation of crystal gardens, a sodium silicate membrane is formed around a crystal of a transition metal salt which is then dissolved by ingress of the solution. As in the crystal garden process, the growth of POM-based tubular architectures appears to be driven by an osmotic pump mechanism, modulated by the rate of water ingress over an initially formed membrane around the crystal. In this work, we set out to extend our study to a variety of POM- and cation-based systems.<sup>25</sup> In general, following the addition of a drop of the aqueous cation solution, the POM crystal begins to dissolve, and aggregation of the POM fragments and cations forms a highly insoluble, yet semi-permeable, membrane around the crystal. Once formed, the membrane effectively isolates the crystal from the surrounding solution. However, water ingress is not prevented, so the encapsulated crystal continues to dissolve. The resulting gradient of concentration causes the formation of an osmotic pump (Figure 3) that draws further molecules of water

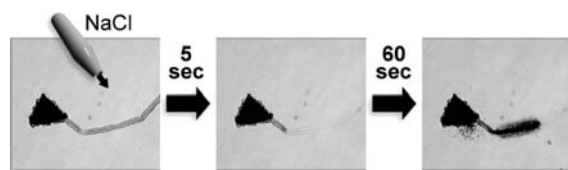


**Figure 4.** Plot of growth rate/crystal surface area against the overall concentration of DIP, showing how the diameter is related to the cation concentration. Red squares show the linear decrease in growth rate as the concentration is decreased, and blue squares show rate data for a tube in which the concentration of DIP is varied while it is growing. Note: The crystal surface area is considered as it relates directly to the limiting rate at which water can enter the membrane surrounding the crystal, and therefore the rate of POM dissolution and tube growth. This allows direct comparison of tubes grown from crystals of varying sizes and shapes.

through the walls of the membrane. Eventually, this results in rupture of the membrane, whereupon POM material is ejected into the cation solution and continuously aggregates to form the wall of a tube, with closure being prevented by the continued flow (see movie 1 showing this process). This sustained flow allows the whole system to sustain a high material flux, which is terminated only by the complete dissolution of the crystal, at which point tube growth ceases. Key differences with the crystal garden system include the fact that, due to the relative density of their components, the tubular architectures usually grow horizontally across the surface (despite the fact that the experiment is carried out in a relatively large volume), whereas convection tends to cause the crystal gardens to grow vertically, and also the fact that the tubular architectures remain open and do not collapse into each other.<sup>10–13</sup> The other major difference is that the controlling concentration of the cation in solution is very low compared to that in crystal gardens, which require more concentrated, sometimes nearly saturated, solutions of sodium silicate.<sup>10–13</sup>

This process could theoretically allow a single tube to propagate until the crystal is entirely consumed, since the flow depletes POM concentration in its neighborhood. This is, however, not the case, and the growth often stops within 2–3 min (although growth can persist for as long as 30 min). This may be due to the pressure in the tube causing a new rupture point, either at the source or somewhere along the tube, in which case tube growth continues from that new rupture point and the original tube ceases to grow. The likelihood of this occurrence is increased when the growing end of the tube encounters an obstruction on the surface. The diameter of a growing tube can be controlled by changing the concentration of cations, and this has been demonstrated in the range 1.5–2.5 mM for cation 1 (see Figure 4). Increasing the cation concentration leads to a decrease of the tube diameter, whereas addition of pure water (to decrease the overall cation concentration) leads to an increase of the tube diameter.<sup>27</sup> In the limiting case, when the cation concentration is raised too far, tube growth will not propagate/initiate because any ruptures in the membrane will be immediately sealed.

These changes can be made in real time, while the tube is still growing, and repeated many times to predictably produce a tube with variable diameter. Once the initial membrane has formed

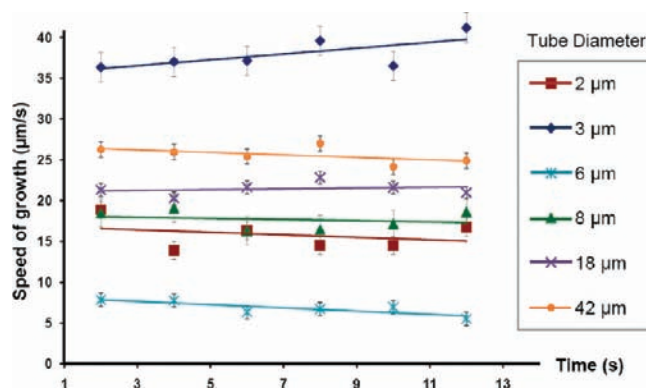


**Figure 5.** Addition of aqueous sodium chloride solution to a growing tube (I/1) causes tube growth to temporarily stop as a competitive osmotic flow is initiated. After equilibration of the sodium chloride concentration across the membrane (30–60 s), tube growth continues, not necessarily on the same path.

around the crystal and tube growth has started, the limiting rate at which water can cross the membrane, and therefore the rate of POM dissolution, becomes fixed and is related directly to the surface area of the membrane. Since the membrane forms on the surface of the crystal, the initial crystal size can be used to estimate the membrane surface area and correct for this effect. The growth rate then varies proportionally with cation concentration over the range where tube growth can occur. Controlling the diameter by changing cation concentration can be explained in terms of the availability of cations to reach a critical level of aggregation required for precipitation of the tube-forming material. The increase in the cation concentration in the neighborhood of a growing tube supplies a greater density of cations, so fragments in the plume of ejected POM material will travel less distance before they encounter sufficient cations to aggregate. Once the solid material is aggregated and becomes part of the tube wall, it is relatively inflexible, so the diameter of the tube decreases. In the reverse scenario, when the cation concentration is reduced, the ejected POM material expands further before the critical aggregation point is reached, so the tube diameter increases. If the concentration of cations is reduced too far, aggregation may occur too far away for fragments to join the walls, and the tube may cease to grow.

The mechanism of tube growth is osmotically driven, and this is clearly seen by the effect of changing the solution ionic strength. When 2–3 drops of a saturated sodium chloride solution in water are added to a system in which tube growth has already initiated, the growth process is temporarily halted (Figure 5). On addition of the brine outside, the ionic strength of the solution is increased to around 0.5 M (13× that of the original cation solution; see Supporting Information for calculation parameters), so the osmotic potential across the membrane is reversed, since the region of lowest ionic strength is now the inside of the membrane surrounding the POM crystal. The salt injection causes a second, competitive osmotic pump to initiate, drawing solution into the membrane surrounding the crystal, through the tubes. This disrupts the osmotic growth mechanism, as no POM material can be ejected against this new flow direction. Competition between the newly added ionic species and the aggregated material in the tube walls leads to local formation of  $\text{POM} \cdot \text{Na}^+_x$  and  $\text{DIP} \cdot \text{Cl}^-_x$  species, which causes some dissolution of the tube walls (see movie 2 showing this process).

Once the concentration of NaCl has equilibrated with the surrounding solution, the original osmotic pump, whereby dissolved POM material is ejected through the tube, becomes predominant once again. The continued presence of NaCl in the solution no longer influences the osmotic potential directly. However, it does change the solubility properties of the components and the aggregate, leading to significantly thicker/less consolidated tube walls (possibly due to ion exchange of the



**Figure 6.** Plot of rate of tube growth against the overall tube length for the system I/1, showing that the rate remains constant after initiation. Error bars show one standard deviation over the samples measured. Data are shown for tubes with diameters ranging from 2 to 42  $\mu\text{m}$ .


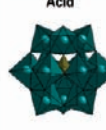
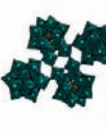
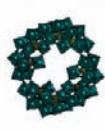


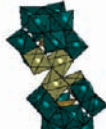
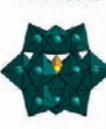

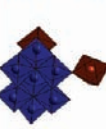
sodium with some of the organocations that form the tubular architecture). Without further perturbation, the system will once again continue the morphogenesis until all the crystalline material is expended.

The reaction to salt addition, and the recovery of tube growth, demonstrates that the growth process can be considered to follow a siphon-like mechanism, in that the concentration of dissolved POM material is maintained along the whole length of the tube. While the POM material remains available in crystalline form, the local concentration of POM material in solution will tend toward saturation, because of the low solubility of the POM. Once a membrane rupture has occurred and tube growth is underway, the ingress of water into the membrane is controlled by the removal of saturated solution from the membrane “chamber” through the tube. This means that the POM material is at saturation along the length of the tube, and as a consequence of this, the rate of tube growth remains constant, even as the tube extends several hundred micrometers from the parent crystal (Figure 6).

The overall solubility of the crystals is critical not only in modulating the rate of tube growth but also in initiating tube growth. When the pH of the overall solution is raised after tube growth initiation, thus modulating the solubility of the POM, the rate of tube growth increases as expected. However, if the pH is raised before tube growth has started, only precipitation is observed, as the crystal dissolves too rapidly for the initial membrane shell to become consolidated.<sup>27</sup> In order to evaluate the limits of POM solubility in the tube initiation/growth phenomenon, 10 different POMs and 8 different cations were selected—polyaromatic molecules and transition metal complexes—to conduct an assay of tube growth. A representation of the different component species is shown in Tables 1 and 2, along with the charges of cations and solubilities of POMs (in water at 20 °C).

The key properties of the POM material that influence the growth of tubes are the size and solubility of the crystal. These govern both the amount of material that can be dissolved from the crystal surface and the rate at which it can aggregate. The size and shape also directly influence the surface area of the membrane, which later controls the rate at which water can enter, and therefore the rate of tube propagation. Temperature and pH can be considered as secondary factors, as they also affect the growth process but do so by modulating the crystal solubility.

Table 1. Polyhedral Representation (Counterions Omitted) of the 10 POM Species Used in the Solubility Experiments<sup>a</sup>

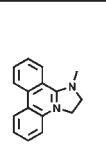
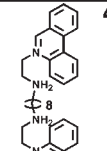
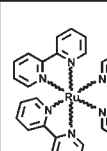
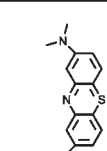
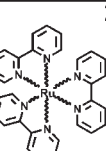
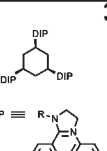
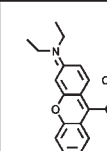
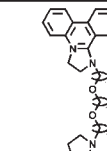
A	B	C	D	E
K <sup>+</sup> salt 	Phosphotungstic Acid 	K <sup>+</sup> salt 	K <sup>+</sup> /Li <sup>+</sup> salt 	Na <sup>+</sup> salt 
720 mg/mL	192 mg/mL	73 mg/mL	37 mg/mL	29 mg/mL
F	G	H	I	J
Na <sup>+</sup> salt 	EMID-salt 	TBA salt 	Morpholinium salt 	HMTA-salt 
9.9 mg/mL	5.9 mg/mL	3.6 mg/mL	3.1 mg/mL	2.0 mg/mL

<sup>a</sup> A,  $K_6[P_2W_{18}O_{62}] \cdot 19H_2O$ ; B,  $[H_3PW_{12}O_{40}] \cdot nH_2O$ ; C,  $K_{24}[P_4W_{52}O_{178}] \cdot 47H_2O$ ; D,  $K_{28}Li_5H_7[P_8W_{48}O_{184}] \cdot 92H_2O$ ; E,  $Na_{15}[(PO_2)_3-PNb_9O_{34}] \cdot 22H_2O$ ; F,  $Na_{22}[Mo^{VI}_{36}O_{112}(H_2O)_{16}] \subset [Mo^{VI}_{130}Mo^{V}_{20}O_{442} \cdot (OH)_{10}(H_2O)_{61}] \cdot 180H_2O$ ; G,  $(C_6H_{11}N_2)_8[(SiW_{10}O_{36})_2(Ni_4O_4)] \cdot 10H_2O$ ; H,  $[[CH_3(CH_2)_3_4N]_4[SiW_{12}O_{40}]]$ ; I,  $(C_4H_{10}NO)_{40}[W_{72}Mn_{12}O_{268}Si_7] \cdot 48H_2O \cdot 4(C_4H_9NO)$ ; J,  $(C_6H_{13}N_4)_2[Fe_2(H_2O)_9Mo_7O_{24}] \cdot 2H_2O$ . Polyhedra are colored to show their metal center's nature: Mo, blue; W, teal; Nb, red; Fe, brown; Ni, light yellow; Mn, purple; Si, golden yellow; P, dark yellow. EMID = 2-ethyl-4-methylimidazolium and HMTA = hexamethylenetetrammonium.

It is important to consider the initial stages of tube growth, as this is the critical time when the membrane shell is formed. If the membrane is weak or the dissolution of the crystal is too rapid, there will not be sufficient containment to produce the required osmotic potential for tube growth. Conversely, tube growth will also not initiate if the aggregated membrane is too strong to be broken by the osmotic pressure within, or if the cation concentration is so high that ruptures are instantly "self-healed".

The properties of the cation must also be considered. In experiments with larger volumes (>1 mL), the solution concentration can be considered as a constant throughout the tube growth. Indeed, even if the tube formation depletes the cations in the medium immediately surrounding the growing end of the tube, the point of growth continuously moves forward into areas where the cations are still present. In experiments conducted in droplets, the concentration change over time becomes more significant, and indeed tube diameter is seen to increase slightly. When a droplet experiment is continuously supplied with fresh cation solution, so as to truly maintain a constant concentration, no change in tube diameter is observed. The cation must also be sufficiently soluble to allow a high enough concentration in the vicinity of the crystal at initiation for aggregation to occur; see Table 3, which describes the crystal/tube initiation results. These data provide a template for the development of a robust predictive methodology for the design of modular tubular architectures. However, it is important that the charge and size of both the cations and anions are considered, as the aggregation process is electrostatically controlled. This is because we have established that the aggregation of POM and cation occurs in a ratio that is expected to result in full charge balancing,<sup>26</sup> and it can

Table 2. Representation of the 8 Cationic Species Used in the Solubility Experiments, Showing Their Charges (Counterions Omitted)<sup>a</sup>

1	2	3	4
			
+	4+	2+	+
5	6	7	8
			
2+	3+	+	2+

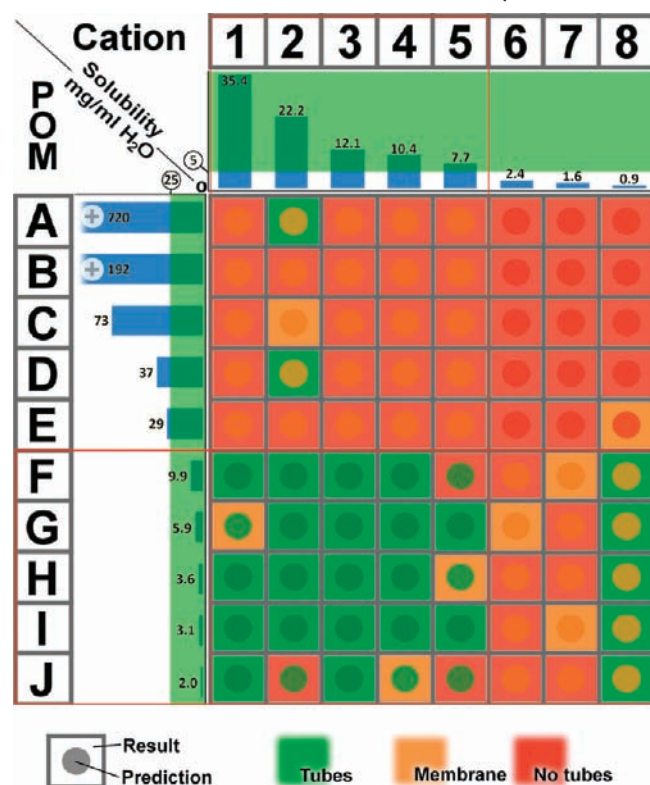
<sup>a</sup> 1, 1-methyl-2,3-dihydro-1H-imidazo[1,2-f]phenanthridin-4-ylum bromide {Me-DIP};<sup>34</sup> 2, *N,N'*-bis(5-phenanthridinium-5-yl-ethyl)octane-1,8-diamine dihydrochloride; 3, (phenanthroline)bis(2,2'-bipyridine)ruthenium(II) ditetrafluoroborate; 4, methylene blue; 5, tris(2,2'-bipyridine)ruthenium(II) dichloride; 6, *cis*-1,3,5-tris(2,3-dihydro-1H-imidazo[1,2-f]phenanthridinium)cyclohexane tribromide; 7, rhodamine B; 8, 1,3-propoxy-DIP-propane dibromide.

be tentatively proposed that this modulates both the porosity of the initial membrane and the thickness of the tube walls. It is also observed that, with the same POM, the use of more highly charged cations gives rise to faster-growing, narrower tubes since a lower local cation concentration is required in order to cause aggregation.

As shown in Table 3, there is a double-threshold effect where the concentration of cations and the solubility of the POM must be "in-range" before tube growth can occur. If the concentration is too high, the initial membrane is formed but then no tube growth is observed, since any ruptures to the membrane are immediately closed. If the cation concentration is too low, POM material dissolves but is able to diffuse too far from the parent crystal before aggregation occurs. No consolidated membrane is formed, but local precipitation is observed. Considering the solubility and tube growth data, the rate of tube growth was investigated for a POM crystal dropped in a solution of cation at a known concentration. To do this, two different POMs, I and G, were selected as they are capable of undergoing morphogenesis with many different cations, and the rates of tube growth with solutions of the original DIP molecule (1), a similar but highly charged dimer (2), and a transition metal complex (5) were measured. The concentrations of the solutions were kept between  $10^{-2}$  and  $10^{-3}$  M, as this gives reliable tube growth with measurable rates, and the results of the average speed of growth versus the initial cation concentration are displayed for POMs I and G in Figure 7.

Two main results can be extracted from these data:

- (1) The more soluble POMs give rise to faster tube growth for any cation.
- (2) For either POM, the most highly charged cations give the fastest growth rates.

Table 3. Presentation of the Tube Growth Assay Results<sup>a</sup>

<sup>a</sup> Green areas shown along the  $x$  and  $y$  axes are the estimated thresholds in which tubes can grow. Using this, we made a prediction of the experiments results: if both POM and cation are in the green solubility area, tubes are expected; if only one of the species is on the limits, membranes are expected; and if neither of them is on the green area, nothing is expected. In terms of the experimental data, green indicates that tubes were observed, orange indicates that membranous material was formed but not in the form of tubes, and red indicates that no tubes or membranous materials were observed.

Data were not adjusted for crystal surface area, but similar sized crystals were chosen for each experiment to avoid surface area effects. The dependence of growth rate on POM solubility stems from the “siphon” mechanism, where the more soluble POM will allow the whole pumping mechanism to operate faster and with a higher osmotic potential. This will cause material to be ejected from the growing tube end at a greater rate. At the growing end of the tube, the cation charge modulates the growth rate because it changes the number of molecules that are required to enter into an electrostatic interaction with the dissolved POMs to produce a neutral aggregate.

Initiation of tube growth requires a sufficient local concentration of cations to be present in order to form the membrane around the POM crystal, and it is therefore not possible to grow tubes under normal conditions in pure water or solutions with very low cation concentration. However, since the process only requires a local availability of cations, it is possible to construct a minimal system where the cations are coated onto the crystal of the POM and are in sufficient concentration to produce tubes. This localization is achieved by depositing a shell of cation material all around the POM crystal using a cation solution in a solvent in which the POM is totally insoluble. The introduction of such a micro-sized core–shell particle into pure water gives

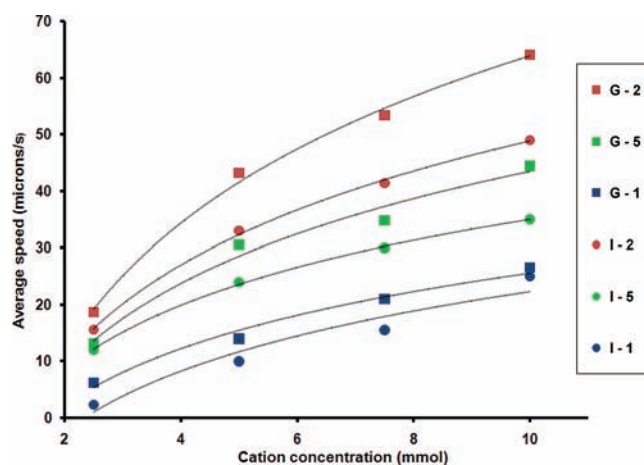
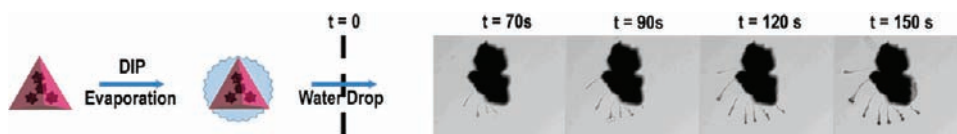


Figure 7. Plot of average speed of growth versus cation concentration for the POMs I and G along with the cations 1, 2, and 5. The rate of growth is clearly higher for the more soluble POM G and more highly charged cations 2 (4+) and 5 (2+).

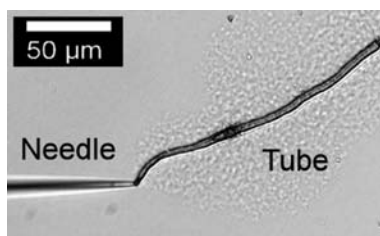
rise to a situation where initial membrane formation is instantaneous, and the remaining cations diffuse around the neighborhood of the crystal. This “seed” then proceeds to grow tubes by the normal mechanism (Figure 8), although due to the limited availability of cations, the membrane around the parent crystal is weak and so several rupture points occur, leading to multiple tubes. The tubes grow rapidly and, as expected, their diameter increases due to the decreasing concentration of cations as the growing end travels farther from the source of cations (precisely the same effect as lowering the cation concentration to control the diameter in previous experiments). Growth continues until the tubes reach a region where there is insufficient cation concentration, after which they remain open and dissolved POM material is continuously expelled until the crystal is expended. Because the tubes remain open and material is pumped out through them, the osmotic pressure is continuously relieved, and further ruptures to the membrane around the parent POM crystal do not occur.

To explore different avenues for the fabrication of the tubular architectures, it was postulated that growth of such tubes could be possible from a narrow aperture involving an extrusion process. To investigate this, crystals of compound I were dissolved in water, and the filtered solution was injected into a cation solution (1) via a 5  $\mu\text{m}$  aperture needle, using a syringe pump. As predicted, it was possible to fabricate 25  $\mu\text{m}$  diameter tubes up to 500  $\mu\text{m}$  in length. Fabrication was possible via extrusion when the needle was both stationary and moving, demonstrating that such tube “drawing” could be used to make pre-designed patterns with tubes (Figure 9). However, the main limitation is once again the solubility, and “writable” tubes require relatively insoluble POM-based materials; injection of the more soluble POMs did not result in the formation of tubes.

It was also suggested that microcrystalline POM materials, formed into a hard pellet under pressure, might also be used to grow tubes, so this was investigated by immersing a pellet derived from powdered compound I into a solution of cation 1. Tube growth was indeed observed, further demonstrating that the crystalline form of the POM is not necessary for growth initiation, although the tubes produced were less stable as those produced from single crystals due to the slightly increased solubility of the POM pellet.



**Figure 8.** Picture describing the seed growth experiment. A crystal of **I** was suspended in a methanolic solution of **1**. After dry evaporation, some cationic molecules were stuck on the crystal, and tube growth was observed whenever it was dropped on pure water.



**Figure 9.** Growth of a tube from a needle. Dissolved POM **I** was injected into a solution of cation **1** via a micromanipulator needle.

## CONCLUSIONS

In conclusion, the spontaneous morphogenesis of crystals of POM-based clusters into tubular architectures by addition of a solution of a cation has been investigated. In this study, both the mechanism of growth and a new methodology for the predictive design of the tubular architectures are presented. It is shown that the tube growth is robust and depends on modular components, whereby the physical properties of the components can be translated into the overall tubular architecture; this is a general phenomenon that is limited only by the solubility of the parent materials. In the initiation phase, if the crystal is too soluble, the formation of the initial membrane will not occur, as POM material will diffuse too rapidly for aggregation with the cations. Conversely, if the POM is not sufficiently soluble, the continued dissolution of the crystal and consequent ingress of water across the membrane, once formed, by osmosis will never reach the critical level required to cause rupture. However, there is little observed interdependency between the solubility of POMs and cations. Instead, a double threshold is observed in the case of the crystalline POM, whereas the solubility of the cation has to be above a certain value in order to have sufficient molecules available in the vicinity of the POM crystal to take part in the initiation of membrane formation and tube aggregation. Any other combinations lead to either failure of the tube formation or plastic-like membrane formation.<sup>28</sup>

Growth rate data show that once tube growth has initiated, and while POM-based material is available at the parent crystal, the concentration of POM fragments in the membrane and along the tube is maintained at saturation. The mechanism of growth can therefore be conceptualized as a “siphon” mechanism, whereby the aggregation of material at the growing end and the ingress of water across the membrane at the crystal are the only limiting factors to growth rate. The data imply that this mechanism is general for any POM and any sufficiently large organic cation or transition metal complex, as long as the POM solubility is within the limits of 1–25 mg/mL. Tube growth rates for different cation/anion combinations reveal that the more soluble POMs give rise to faster tube growth, regardless of cation, while for a given POM, the most highly charged cations will give the fastest growth rates. Further, the osmotic mechanism is underlined by the fact that non-active salt addition leads to an

immediate stop of the tube growth by reversing the osmotic potential across the membrane.

By defining the solubility limits of tube growth and translating these into a predictive methodology, it is now possible to predict whether given POM/cation combinations can undergo morphogenesis to produce tubular architectures. This has also given insights regarding manipulations on the limits of the phenomenon. For example, it was shown that the solid and precisely ordered form of the crystalline POM is not essential for tube growth, as a tube can be fabricated by extruding dissolved POM material from a needle, or from a pellet of powdered POM material. This new method of tube synthesis may allow morphogenesis to tubes from POM materials which are difficult to crystallize in a convenient time scale. Also, by stripping away the unnecessary components to make a tube-growing “seed”, a “minimal self-growing system” was achieved, to which various physicochemical properties could be functionalized.

In this work we have established a new phenomenon, the growth of hollow mineral tubular architectures, and this may have significance in the interpretation of architectures found in the fossil record that have been thus far attributed to biological processes.<sup>29</sup> For example, microtube architectures have been reported containing organic residue that have been postulated to be one of the earliest life-forms present on planet Earth. However, it has been shown in this work that microtubes can spontaneously form “naturally” if the correct oxides and cations come into contact. Therefore, the assumption that microtubes imply life is no longer valid in isolation.<sup>30</sup> In future work we will take advantage of the use of the transition metal complexes and especially those based on ruthenium to undergo catalysis, such as water oxidation. The use of one-pot-synthesized POM species to catalyze water oxidation is now well described in the literature and could be adapted to this tubular system, with the advantages of the retrieval of the catalyst and also the ability to grow tubes into complex patterns for catalytic device manufacture. Further work will seek to expand on the modularity emphasized here, by producing new POM-based tubular architectures that show catalytic and functional properties associated with their precursor materials.

## EXPERIMENTAL SECTION

**Sample Preparations.** The different POMs were synthesized according to the published literature.<sup>24,31–33</sup> Materials in crystalline form were collected directly from the bulk synthesis and dried under vacuum. Commercially available cations and transition metal complexes were purchased from Sigma-Aldrich Ltd. and used without further purification. The DIP derivatives were synthesized following the procedures reported earlier by our group.<sup>34</sup> Solutions of fixed concentrations, typically  $1 \times 10^{-2} \text{ mol} \cdot \text{L}^{-1}$ , were prepared by dissolving the correct amount of dry material in 10 mL of water, and solutions of lower concentration were prepared by dilution.

**Synthesis for Cation 2.** To 5-(2-bromoethyl)-phenanthridinium bromide (BEP) (2 equiv, 2.77 mmol, 1.02 g) and 1,8-diaminooctane (1 equiv, 1.39 mmol, 200 mg) were added dichloromethane (DCM,

80 mL) and 5% Na<sub>2</sub>CO<sub>3</sub> (40 mL), and the resulting biphasic solution was stirred for 4 h at room temperature. The organic layer was removed and washed with water, HCl (1 M) was added, and the mixture was stirred for 90 min. Both layers were then concentrated to give a pale yellow powder, which was dissolved in water and transferred to a separating funnel along with DCM and Na<sub>2</sub>CO<sub>3</sub> (all in equal volumes), forming a creamy suspension in the upper aqueous layer. The DCM was removed and replaced with CHCl<sub>3</sub> with the same outcome. Both organic layers were combined and extracted into HCl, after which the aqueous layer was concentrated, giving a pale yellow residue. Ethyl acetate was added to the aqueous layer from the DCM wash, forming a brown upper layer which was removed and extracted into HCl. This final HCl solution was concentrated, giving the final product **2**. Analytical details can be found in the Supporting Information.

**General Microscope Measurements.** Experiments were conducted at room temperature and under air using plastic well or glass slides with an Olympus IX81 inverse microscope. Images were taken, analyzed, and processed through the Cell<sup>R</sup> software.

**Typical Rate of Growth Experiment.** Five milligrams of crystalline POM material was deposited on the bottom of a dry plastic well. Next, 0.5 mL of the cation-containing solution was added at  $t = 0$  s, and time lapse images (focused to the bottom of the well) were recorded every few seconds. The rate of growth was measured by image analysis on focused growing tubes for each system. Time lapse of one image per 2 s for 50 frames proved to be convenient. However, in the case of low concentrations such as  $2.5 \times 10^{-3}$  mol·L<sup>-1</sup> and/or slow systems, time lapse of every 5 s for 50 frames was used.

## ■ ASSOCIATED CONTENT

**S Supporting Information.** Details of the equipment and experiments, tables of growth rate data, synthesis of **2**, and relevant pictures. This material is available free of charge via the Internet at <http://pubs.acs.org>.

**W Web Enhanced Feature.** Two videos, in .avi format, are available in the HTML version of this paper. Movie 1 shows a tubular architecture growing from a crystal of POM covered by a drop of an aqueous solution containing organic cations. Movie 2 shows the effect of adding NaCl solution to a growing tube system. The tube growth ceases and back-flow of material is observed. After a lag time during which the salt concentration equilibrates, tube growth starts again.

## ■ AUTHOR INFORMATION

### Corresponding Author

L.Cronin@chem.gla.ac.uk

## ■ ACKNOWLEDGMENT

This work was supported by the EPSRC, University of Glasgow, and WestCHEM. L.C. thanks the Royal Society/Wolfson Foundation for a merit award.

## ■ REFERENCES

- (1) Banfield, J. F.; Welch, S. A.; Zhang, H.; Ebert, T. T.; Penn, R. L. *Science* **2000**, *289*, 751–754.
- (2) Liu, T. B.; Diemann, E.; Li, H. L.; Dress, A. W. M.; Mueller, A. *Nature* **2003**, *426*, 59–62.
- (3) Capito, R. M.; Azeveo, H. S.; Velichko, Y. S.; Mata, A.; Stupp, S. L. *Science* **2008**, *319*, 1812–1816.
- (4) Zhang, J.; Song, Y. S.; Cronin, L.; Liu, T. B. *J. Am. Chem. Soc.* **2008**, *130*, 14408–14409.

- (5) Taft, K. L.; Papaefthymiou, G. C.; Lippard, S. J. *Inorg. Chem.* **1994**, *33*, 1510–1520.
- (6) Maselko, J.; Strizhak, P. *J. Phys. Chem. B* **2004**, *108*, 4937–4939.
- (7) Chichak, K. S.; Cantrill, S. J.; Pease, A. R.; Chiu, S.-H.; Cave, G. W. V.; Atwood, J. L.; Fraser Stoddart, J. *Science* **2004**, *304*, 1308–1312.
- (8) Cairns-Smith, A.-G. *Chem. Eur. J.* **2008**, *14*, 3830–3839.
- (9) Yang, L. F.; Dolnik, M.; Zhabotinsky, A. M.; Epstein, I. R. *Phys. Rev. E* **2000**, *62*, 6414–6420.
- (10) Collins, C.; Zhou, W.; Mackay, A. K.; Klinowski, J. *Chem. Phys. Lett.* **1998**, *286*, 88–92.
- (11) Cartwright, J. H. E.; Garc -Ruiz, J. M.; Novella, M. L.; Ot lora, F. *J. Colloid Interface Sci.* **2002**, *256*, 351–359.
- (12) Thouvenel-Romans, S.; Steinbock, O. *J. Am. Chem. Soc.* **2003**, *125*, 4338–4341.
- (13) Makki, R.; Al-Humiari, M.; Dutta, S.; Steinbock, O. *Angew. Chem. Int. Ed.* **2009**, *48*, 8752–8756.
- (14) Katsoulis, D. E. *Chem. Rev.* **1998**, *98*, 359–387. Yamase, T. *Chem. Rev.* **1998**, *98*, 307–325. Kozhevnikov, I. V. *Chem. Rev.* **1998**, *98*, 171–198.
- (15) Rhule, J. T.; Neiwert, W. A.; Hardcastle, K. I.; Do, B. T.; Hill, C. L. *J. Am. Chem. Soc.* **2001**, *39*, 1772–1774.
- (16) Zeng, H. D.; Newkome, G. R.; Hill, C. L. *Angew. Chem. Int. Ed.* **2000**, *39*, 1772–1774.
- (17) Ogliao, F.; de Visser, S. P.; Cohen, S.; Sharma, P. K.; Shaik, S. J. *Am. Chem. Soc.* **2002**, *124*, 2806–2817.
- (18) Streb, C.; Ritchie, C.; Long, D. L.; K gerler, P.; Cronin, L. *Angew. Chem. Int. Ed.* **2007**, *46*, 7579–7582.
- (19) Rhule, J. T.; Hill, C. L.; Judd, D. A. *Chem. Rev.* **1998**, *98*, 327.
- (20) Yan, J.; Long, D.-L.; Miras, H. N.; Cronin, L. *Inorg. Chem.* **2010**, *49*, 1819–1825.
- (21) Long, D.-L.; Kogerler, P.; Farrugia, L. J.; Cronin, L. *Angew. Chem. Int. Ed.* **2003**, *42*, 4180.
- (22) Long, D.-L.; Abbas, H.; Kogerler, P.; Cronin, L. *J. Am. Chem. Soc.* **2004**, *126*, 13880.
- (23) Long, D.-L.; Kogerler, P.; Parenty, A. D. C.; Fielden, J.; Cronin, L. *Angew. Chem. Int. Ed.* **2006**, *45*, 4798.
- (24) Miras, H. N.; Cooper, G. J. T.; Long, D.-L.; B gge, H.; M ller, A.; Streb, C.; Cronin, L. *Science* **2010**, *327*, 72–74.
- (25) Ritchie, C.; Streb, C.; Thiel, J.; Mitchell, S. G.; Miras, H. N.; Long, D.-L.; Boyd, T.; Peacock, R. D.; McGlone, T.; Cronin, L. *Angew. Chem. Int. Ed.* **2008**, *47*, 6881.
- (26) Ritchie, C.; Cooper, G. J. T.; Song, Y.-F.; Streb, C.; Yin, H.; Parenty, A. D. C.; MacLaren, D. A.; Cronin, L. *Nature Chem.* **2009**, *1*, 47.
- (27) Cooper, G. J. T.; Cronin, L. *J. Am. Chem. Soc.* **2009**, *131*, 8368–8369.
- (28) Cooper, G. J. T.; Kitson, P. J.; Winter, R.; Long, D.-L.; Cronin, L. Manuscript in preparation.
- (29) Furnes, H.; Banerjee, N. R.; Muehlenbacks, K.; Staudigel, H.; de Wit, M. *Science* **2004**, *304*, 578–581.
- (30) Mcloughlin, N.; Staudigel, H.; Furnes, H.; Eickmann, B.; Ivarsson, M. *Geobiology* **2010**, *8*, 245–255.
- (31) Contant, R.; T z , A. *Inorg. Chem.* **1985**, *24*, 4610–4614.
- (32) Pradeep, C. P.; Long, D.-L.; Streb, C.; Cronin, L. *J. Am. Chem. Soc.* **2008**, *130*, 14946–14947.
- (33) Nyman, M.; Celestian, A. J.; Parise, J. B.; Holland, G. P.; Alam, T. M. *Inorg. Chem.* **2006**, *45*, 1043–1052.
- (34) Parenty, A. D. C.; Smith, L. V.; Pickering, A. L.; Long, D.-L.; Cronin, L. *J. Org. Chem.* **2004**, *69*, 5934.